

# Empirical Data Modeling of Power Converters

J.Y. Choi and I. Choy,  
Korea Institute of Science and Technology, Seoul, Korea  
B.H. Cho  
Seoul National University, Seoul, Korea  
and  
H.F. VanLandingham  
Virginia Polytechnic Institute and State University  
Blacksburg, Virginia, USA

**Abstract** This paper addresses the topic of modeling of highly nonlinear power electronics systems. As an application of identifying an unknown plant in power electronics systems, an empirical data modeling approach is presented which aims at generating discrete-time small-signal linear equivalent models for a general class of converters, which includes resonant and PWM type converters. The resulting small-signal model describes the converter as a linear time invariant system, and the knowledge of the identified linear system can be applied to the switching converters for constructing feedback controllers. The identification results are compared with the analytical model and experimental data.

## I. INTRODUCTION

Switching converters are inherently nonlinear oscillatory systems. A switching converter consists of linear resistors, inductors, capacitors, as well as nonlinear magnetic components and semiconductor switches. Especially, due to the severe nonlinear characteristics of magnetic components and switching devices, it is very difficult to design stable feedback controllers using exact mathematical descriptions of switching converters. Usually, switching converters have too many complex nonlinear differential equations to be solved. Therefore, it is generally not feasible to construct design guidelines to regulate a converter in a large-signal domain. Instead, small-signal models are commonly used to provide dynamic information of the switching converters for control purposes, where the converter can be linearized around a specific operating point. Since the control issues of switching converters can be treated very

effectively by small-signal analysis, the resulting small-signal models are very useful to design engineers on the ground that all of the relatively simple techniques of linear system control theory can be applied easily to the small-signal model. Therefore, practicing engineers may acquire the physical insight of the given system for developing a proper feedback controller. From this small-signal model important specifications such as audio susceptibility, loop-gain and output impedance are calculated. Additionally, these specifications can be easily measured whenever the small-signal model and/or the controller based on this model needs to be verified experimentally.

For the past decades, state-space averaging is a commonly used modeling approach for small-signal modeling of switching converters. This method was originally proposed to model PWM converters. For properly designed PWM converters, the natural frequencies of each linear circuit are much lower than the switching frequency. This provides justification of the linear ripple assumption. Under the assumption that the natural frequency of the converter power stage is well below the switching frequency, the averaging technique can provide approximate linear solutions of a nonlinear averaged state equation. Then, the small-signal model can be derived by "persistently exciting" input signals around a particular operating point. The obtained small-signal model has a continuous form. The model can predict the dynamics of PWM type converter power stages accurately up to the half of the switching frequency. The analysis of state-space averaging is simplified by using a circuit averaging technique based on three-terminal PWM switch model [1]. However, this averaging concept does not apply for resonant converters and multi-resonant converters where the

energy of state variables is carried mainly by switching harmonics but not by the low frequency components as in the case of PWM type converters. For resonant converters and multi-resonant converters, the dynamics are often determined by the interaction between the switching frequency and the natural resonant frequency of the converter [2]. This interaction cannot be investigated using averaging concept because it eliminates the switching frequency information.

Another systematic modeling method to obtain small-signal models for switching converters is a discrete-time (D-T) or a sampled-data modeling approach. By solving the nonlinear state equations in the time-domain, a steady-state analysis can be done under given operating conditions. Perturbation of this nonlinear equation around a specific operating point provides the small-signal dynamics with a sample interval the same as the switching frequency.

In this paper, small-signal modeling of a PWM type boost converter and a series-resonant converter to apply the identification technique. This empirical data modeling approach is generally simpler and independent of type of converters. Also, since this approach is a model-free identification, internal structure need not be known as long as one can obtain the data either through a time-domain simulation or a hardware measurement. This approach is also very effective to generate a reduced order model to represent a complex subsystem in a distributed power system.

## II. SYSTEM IDENTIFICATION

In his often referenced paper [3] Luenberger established nominal structures for a multi-input, multi-output (MIMO) system. The method is based on the concept of either controllability or observability indices. For present purposes only the observability form will be discussed. Beginning with an assumed D-T state space model,

$$\begin{aligned} \mathbf{x}(k+1) &= \mathbf{A}\mathbf{x}(k) + \mathbf{B}\mathbf{u}(k), & \mathbf{x}(0) \\ \mathbf{y}(k) &= \mathbf{C}\mathbf{x}(k) + \mathbf{D}\mathbf{u}(k) \end{aligned} \quad (1)$$

where  $\mathbf{x}$  is an  $(n \times 1)$  vector,  $\mathbf{u}$  is an  $(m \times 1)$  vector,  $\mathbf{y}$  is a  $(p \times 1)$  vector and the matrices  $\mathbf{A}$ ,  $\mathbf{B}$ ,  $\mathbf{C}$  and  $\mathbf{D}$  have corresponding compatible dimensions, the observability matrix is given by the matrix  $\mathbf{Q}_o$ ,

$$\mathbf{Q}_o = [ (\mathbf{c}_1)^T \dots (\mathbf{c}_p)^T \mid (\mathbf{c}_1\mathbf{A})^T \dots (\mathbf{c}_p\mathbf{A})^T \mid \dots \mid (\mathbf{c}_1\mathbf{A}^{v-1})^T \dots (\mathbf{c}_p\mathbf{A}^{v-1})^T ]^T \quad (2)$$

The dimensions of  $\mathbf{Q}_o$  are  $(np \times n)$ . For an observable system  $\mathbf{Q}_o$  must have rank  $n$  and, therefore,  $n$  linearly independent rows. The Luenberger form identifies the first  $n$  linearly independent rows from the top. The *observability index* for the pair  $\{\mathbf{A}, \mathbf{C}\}$  is the smallest integer,  $v$ , such that

$$\text{rank}[\mathbf{C}^T \ \mathbf{A}^T\mathbf{C}^T \ \dots \ (\mathbf{A}^T)^{v-1}\mathbf{C}^T] = n \quad (3)$$

*Observability indices* (plural) are defined as the set of integers  $\{v_i\}$ ,  $1 \leq i \leq p$ , identifying the lengths of the chains of each row of  $\mathbf{C}$ . For instance, the rows generated by row  $i$  are linearly independent up to (and including)  $\mathbf{c}_i\mathbf{A}^{v_i-1}$ . As an aid to the discussion, the crate diagram is introduced as a means of visualizing which  $n$  linearly independent rows of  $\mathbf{Q}_o$  are being chosen [4]. As an example of a 3-output system of order 7, consider Fig. 1.

	$\mathbf{c}_1$	$\mathbf{c}_2$	$\mathbf{c}_3$	
	1	1	1	$\mathbf{A}^0$
	1	1	0	$\mathbf{A}^1$
	0	1		$\mathbf{A}^2$
		1		$\mathbf{A}^3$
		0		$\mathbf{A}^4$

Fig. 1. Example of a Crate Diagram

In this case the matrix of selected rows,  $\mathbf{T}$ , becomes

$$[\mathbf{c}_1^T \ \mathbf{c}_2^T \ \mathbf{c}_3^T \ (\mathbf{c}_1\mathbf{A})^T \ (\mathbf{c}_2\mathbf{A})^T \ (\mathbf{c}_2\mathbf{A}^2)^T \ (\mathbf{c}_2\mathbf{A}^3)^T]^T \quad (4)$$

Note the correspondence between the partitions of  $\mathbf{T}$  in Eq.(4) and the units in the crate diagram of Fig. 1. Using  $\mathbf{T}$  as a similarity transformation matrix results in the equivalent state space model given by  $\mathbf{A}_o = \mathbf{T}\mathbf{A}\mathbf{T}^{-1}$ ,  $\mathbf{B}_o = \mathbf{T}\mathbf{B}$ ,  $\mathbf{C}_o = \mathbf{C}\mathbf{T}^{-1}$  and  $\mathbf{D}_o = \mathbf{D}$ . This representation is in the *pseudo-observability form (POF)* state space model corresponding to the indices  $\{2,4,1\}$ , as indicated by the number of units in the three columns of the crate. The structure of the

model is illustrated in the  $A_o$  and  $C_o$  matrices described below. The matrix  $B_o$  has no particular structure.

$$A_o = \begin{bmatrix} 0 & 0 & 0 & 1 & 0 & 0 & 0 \\ 0 & 0 & 0 & 0 & 1 & 0 & 0 \\ x & x & x & x & x & x & x \\ x & x & x & x & x & x & x \\ x & x & x & x & x & x & x \\ 0 & 0 & 0 & 0 & 0 & 1 & 0 \\ 0 & 0 & 0 & 0 & 0 & 0 & 1 \end{bmatrix}$$

and

$$C_o = \begin{bmatrix} 1 & 0 & 0 & 0 & 0 & 0 & 0 \\ 0 & 1 & 0 & 0 & 0 & 0 & 0 \\ 0 & 0 & 1 & 0 & 0 & 0 & 0 \end{bmatrix} \quad (5)$$

The matrix  $A_o$  contains the remaining rows of the  $7 \times 7$  identity matrix in rows 1, 2, 5 and 6. Its other rows may have arbitrary elements. The difference between a POF and the corresponding Luenberger form is that Luenberger re-ordered the selected rows by the columns of the crate before performing the similarity transformation, a step which is not only unnecessary, but counter productive in that the resulting structure is more complex!

The idea behind the POFs is that the selection of the  $n$  linearly independent rows of  $Q_o$  can be done in many ways, according to the indices  $\{n_1, n_2, \dots, n_p\}$ , representing the number of units in the  $p$ -columns of the crate. The indices must, of course, sum to  $n$ . Each possibility must be checked for "admissibility," i.e. that the resulting  $n$ -rows are, in fact, linearly independent. The admissible POFs are then all possible structures for the MIMO system. Investigation of the various POFs for a particular system quickly indicates that some forms are better than others in terms of the condition number of the transformation matrix  $T$ . A poorly conditioned transformation matrix typically results in a large range of parameter values in the POF, as well as loss of numerical accuracy in the model.

In Section III the deterministic identification algorithm is reviewed [5]. The identification technique presented in this paper, modified to accommodate noisy data, is given in Section IV.

### III. DETERMINISTIC IDENTIFICATION

In Section II the POF was introduced. The key is in the set of indices specified for the POF in that everything related to the system structure is determined from them. In practice it is useful to establish an algorithm which will construct the POF given a basic state space model and the information of the indices. The reader is referred to Reference [5] for details.

System identification from input/output data assumes that the input signals are "persistently exciting," i.e. that the system is sufficiently excited to exhibit all of its modes in the corresponding output signals. In addition, it is clear that only the controllable and observable part of the system can be identified from input/output data. To develop the necessary background, consider the desired result of the identification, namely, an order- $n$  D-T system with  $m$ -inputs and  $p$ -outputs:

$$\begin{aligned} \mathbf{x}(t+1) &= A_o \mathbf{x}(t) + B_o \mathbf{u}(t) \\ \mathbf{y}(t) &= C_o \mathbf{x}(t) + D_o \mathbf{u}(t) \end{aligned} \quad (6)$$

where  $R_o = \{A_o, B_o, C_o, D_o\}$  is in a POF corresponding to a set of admissible POI,  $v = \{v_i\}$ . From Eq.(6) we may write

$$\begin{bmatrix} \mathbf{y}(t) \\ \mathbf{y}(t+1) \\ \vdots \\ \mathbf{y}(t+r) \end{bmatrix} = \begin{bmatrix} C_o \\ C_o A_o \\ \vdots \\ C_o A_o^r \end{bmatrix} \mathbf{x}(t) + \begin{bmatrix} D_o & \dots & 0 & 0 \\ C_o B_o & \dots & 0 & 0 \\ \vdots & & & \\ C_o A_o^{r-1} B_o & \dots & C_o B_o & D_o \end{bmatrix} \begin{bmatrix} \mathbf{u}(t) \\ \mathbf{u}(t+1) \\ \vdots \\ \mathbf{u}(t+r) \end{bmatrix} \quad (7)$$

Now we let  $r = v = \max\{v_i\}$ . Clearly, Eq.(7) holds for any integer  $t = [0, N-r]$  and can be rewritten as

$$\mathbf{y}_t = Q_{oo} \mathbf{x}(t) + H \mathbf{u}_t \quad (8)$$

where  $\mathbf{y}_t$  and  $\mathbf{u}_t$  are  $(v+1)p$  and  $(v+1)m$  dimensional columns containing output and input vectors  $\mathbf{y}(t+j)$  and  $\mathbf{u}(t+j)$ ,  $j = [0, v]$ . The matrix  $Q_{oo}$  is the observability matrix of the pair  $\{A_o, C_o\}$ , while  $H$  is the  $(r+1)p \times (r+1)m$  lower block triangular matrix containing along the main diagonal the  $(p \times m)$  blocks  $D_o$ . The other nonzero blocks of  $H$  are the  $pxm$



$$[N_r | A_r] = Y_2 Z^T (Z Z^T)^{-1} \quad (17)$$

Using the natural structure described above, the POF realization  $R_o$  can be constructed from the result of Eq.(17). In the next section the technique for system identification is explained.

#### IV. MODELLING OF BOOST CONVERTER AND SERIES RESONANT CONVERTER

As an example of the small-signal modelling of nonlinear dynamic systems under study, an open-loop boost converter and a series resonant converter (SRC) are selected. Since existing state-space averaged model is quite accurate up to the half of the switching frequency, the proposed modelling approach can be compared and verified its effectiveness and accuracy.

##### A. Open-Loop Boost Converter

Fig. 1 illustrates a typical two-state boost converter example.

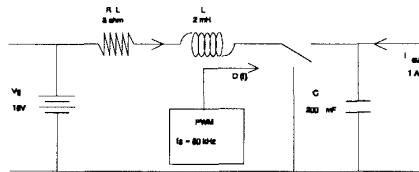


Fig. 1. Boost Converter (with PWM Control over the Switch)

Three input variables and two output variables represent the state of the system dynamics:  $\hat{v}_g$  (the variation of input voltage),  $\hat{i}_o$  (the variation of input current), and  $\hat{d}$  (the variation of duty cycle),  $\hat{i}_l$  (the variation of output inductor current),  $\hat{v}_c$  (the variation of output capacitor voltage). This converter was designed to operate at a nominal duty ratio of 0.6 with an efficiency of 70.5%. The exact discrete state-space equation including all the nonlinearities are used for the time-domain simulation.

As described in detail Reference [6], the modeling procedure is summarized as follows:

Step 1: A small range of elaborate input

perturbations around a nominal equilibrium point is injected at the inputs of the boost converter, such as,  $\hat{v}_g$ ,  $\hat{i}_o$  and  $\hat{d}$ , and then the corresponding output responses are measured in physical unit. Generally, small-signal modeling of an unknown system, unlike the above boost converter, must be done using a circuit simulation tool such as SPICE or the measurement data from the hardware directly. Therefore, extracting information from data is not a straightforward task. In addition to the decisions required for model structure selection and generalization, the collected data need to be handled carefully for the robust identification process. The levels in these raw inputs and outputs should be matched in a consistent way. The mean levels must be subtracted from the input and output sequences before the estimation. The best way is to match the mean levels corresponding to a system equilibrium.

Step 2: The second step is to determine a nominal range of the system order with the restriction that the input signals are "persistently exciting." From the assumption that the order of the system is unknown, to determine the system order from raw data, a rank test is done. However, due to the nonlinearity of the system with added noise, a rank test may not be reliable.

Step 3: The third step is to construct an ARMA model with inputs representing both the present inputs and delayed versions of the inputs and outputs to capture the dynamics of the systems. The method is determining an equilibrium point to identify a linearized system about this equilibrium point. A classical method of multivariable system identification which utilizes the possible structures of the system in order to achieve a model that optimally generalizes over the available input/output data.

Step 4: The final step, a deterministic D-T system identification, is performed by calculating an observable form state-space model  $R_o = \{A, B, C, D\}$  from the identified ARMA model. The small-signal modeling process is shown in Fig. 2

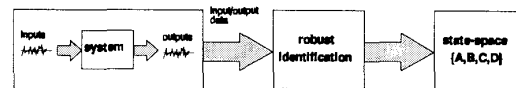


Fig. 2. Small-Signal Modeling Process

Using the proposed identification technique, a small-signal model of the boost converter is developed as

the following ARMA model:

$$y(k) = \sum_{i=1}^n a_i y(k-i) + \sum_{i=0}^n b_i u(k-i) \quad (18)$$

where  $y_1 = \hat{i}_1$ ,  $y_2 = \hat{v}_c$ ,  $u_1 = \hat{v}_g$ ,  $u_2 = \hat{i}_0$  and  $u_3 = \hat{d}$ . From Eq. (18) it is noted that delayed inputs and outputs contribute to the "predicted" output. Since the boost converter is second order, the ARMA model of the linearized system is expected to have  $u_1(k)$ ,  $u_1(k-1)$ ,  $u_2(k)$ ,  $u_2(k-1)$ ,  $u_3(k)$ ,  $u_3(k-1)$ ,  $y_1(k-1)$  and  $y_2(k-1)$  terms. For reference, the eigenvalues of the C-T equivalent model of Eq. (18) are  $\{-1166.6, -347.5\}$  comparing with those of state-space averaged model of the exact system equation,  $\{-1153.1, -346.9\}$ . When duty cycle,  $\hat{d}$ , is modulated, the magnitude and the phase of the control-to-output transfer function of the identified model are compared against the state-space averaged model of the system in Figs. 3 and 4, respectively. The obtained small-signal model is accurate up to the half of the switching frequency, i.e. 25KHz (Nyquist frequency).

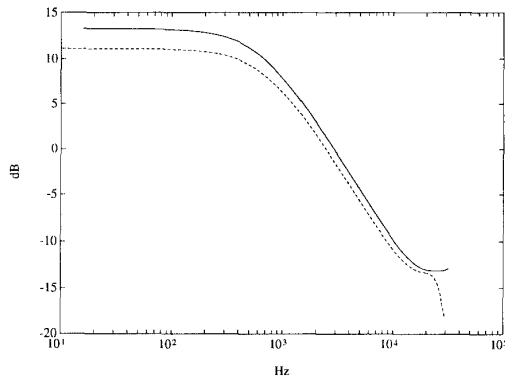


Fig. 3. Magnitude: Identified (solid), State-Space Averaging (dotted)

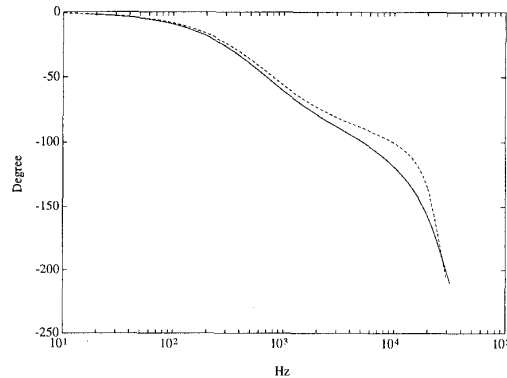


Fig. 4. Phase: Identified (solid), State-Space Averaging (dotted)

### B. Series-Resonant Converter (SRC)

The small-signal modeling approach for a series-resonant converter (SRC) based on the proposed robust hybrid identification technique is discussed in this section. Among several approaches for modeling a SRC, the well-known state-space averaging technique does not show promising results in modeling for resonant converters, where the energy of the system is carried mainly by the switching frequency harmonics (not by the low frequency components as in the case of PWM converters). Since the dynamics are often determined by the interaction between the switching frequency and the natural frequency of the resonant converter, state-space averaging eliminates the useful information of this interaction between both frequencies. Therefore, the previous identification procedure was applied to the input/output data streams of nonlinear system equations of a SRC [6]. The identified model was compared with the analytical result to verify the correctness of the procedure. Figs. 5 and 6 show the control-to-output transfer function of the SRC compared against the measured data. The numerical results are in good agreement with the measured data.

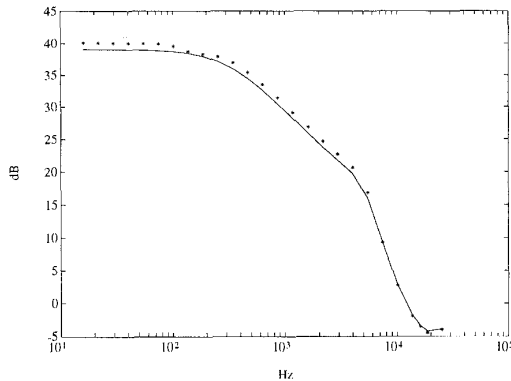


Fig. 6. Magnitude:  
Identified (solid), Measured (\*)

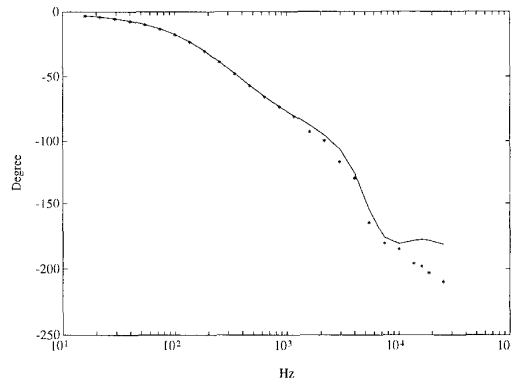


Fig. 7. Phase:  
Identified (solid), Measured (\*)

- [4] Kailath, T., *Linear Systems*, Prentice-Hall, Inc., Englewood Cliffs, NJ, 1980.
- [5] Bingulac, S. and H.F. VanLandingham, *Algorithms for Computer-Aided Design of Multivariable Control Systems*, Marcel Dekker, Inc. New York, NY, 1993.
- [6] J.Y. Choi, "Nonlinear system identification and control using neural networks," *Ph.D. Thesis*, VPISU, Blacksburg, VA, 1994.

#### REFERENCES

- [1] V. Vorperian, "Simplified analysis of PWM converters using the model of the PWM switch: Part I and II," *IEEE Trans. AES.*, vol. 26, no. 3, pp. 490-505, 1990.
- [2] V. Vorperian and S. Cuk, "Small-signal analysis of resonant converters," *IEEE PESC.*, pp. 269-282, 1983.
- [3] Luenberger D.G., "Canonical forms for linear multivariable systems," *IEEE Trans. on Automatic Control*, **AC-12**, 290-293, 1967.